Deep electron traps and origin of *p*-type conductivity in the earth-abundant solar-cell material Cu_2ZnSnS_4

Dong Han,[1,2] Y. Y. Sun,[1,*] Junhyeok Bang,[1] Y. Y. Zhang,[1] Hong-Bo Sun,[2] Xian-Bin Li,[2] and S. B. Zhang[1,2,†]
[1]*Department of Physics, Applied Physics, and Astronomy, Rensselaer Polytechnic Institute, Troy, New York 12180, USA*
[2]*State Key Laboratory on Integrated Optoelectronics, College of Electronic Science and Engineering, Jilin University, Changchun 130012, China*

(Received 8 December 2012; published 15 April 2013)

Using hybrid functional calculation, we identify the key intrinsic defects in Cu_2ZnSnS_4 (CZTS), an important earth-abundant solar-cell material. The Sn-on-Zn antisite and the defect complex having three Cu atoms occupying a Sn vacancy are found to be the main deep electron traps. This result explains the optimal growth condition for CZTS, which is Cu poor and Zn rich, as found in several recent experiments. We show that, under the growth condition that minimizes the deep traps, Cu vacancy could contribute the majority of hole carriers, while the Cu-on-Zn antisite will become the dominant acceptor if the growth condition favors its formation.

DOI: 10.1103/PhysRevB.87.155206 PACS number(s): 84.60.Jt, 61.72.−y, 71.55.−i

I. INTRODUCTION

Cu_2ZnSnS_4 (CZTS) is a semiconductor for making low-cost thin-film solar cells.[1–12] It has the potential to overcome the limitations of other well-known thin-film solar-cell materials, such as $CuIn_xGa_{1-x}Se_2$ (CIGS), in production capacity. Because the expensive group-III elements in CIGS are replaced with the group-IIB element Zn and the group-IV element Sn, all the constituent elements in CZTS are earth-abundant and nontoxic. In addition, CZTS has a direct band gap of about 1.5 eV,[1,4] which is ideal for solar-cell applications. Recently, CZTS has become a celebrated solar-cell material due to remarkable breakthroughs on the power conversion efficiency (PCE), which has reached 8.4% for solar cells based solely on CZTS and 11% for those incorporating selenium.[13,14] To further improve the performance of CZTS-based solar cells, it is critically important to develop systematic understandings on the properties of this material, particularly its defect properties, such as the intrinsic shallow and deep defects, which determine the level of self-doping and the rate of nonradiative recombination of photo-excited carriers, respectively.

Given the large number of possible defects in a quaternary compound, direct identification of the important defects in CZTS by experiment is difficult. One may consider borrowing the understandings on the structurally similar I-III-VI_2 solar-cell materials, such as $CuInSe_2$ (CIS), which have been extensively studied. For CIS, the native *p*-type conductivity was attributed to Cu vacancies (V_{Cu}) and the high PCE achieved by using low-quality thin films was explained based on the finding that the low-formation-energy defects were electrically benign without forming deep levels in the band gap.[15] However, it is not clear to what extent such understandings on CIS still hold true for CZTS. For example, recent first-principles studies have suggested that the native *p*-type conductivity of CZTS is due to the Cu-on-Zn antisites (Cu_{Zn}).[16,17] Moreover, a number of low-formation-energy defects in CZTS were found to exhibit deep levels in the band gap[16] that could be detrimental to the solar-cell performance.

The previous theoretical results point to several fundamental issues, which are critical for planning the strategy of further improving the PCE of CZTS-based solar cells. First, in the first-principles calculations the Cu_{Zn} antisite always had negative formation energy, indicating that CZTS is a metastable material. Second, there is a lack of microscopic understanding why the Cu-poor and Zn-rich condition, which was found to be the optimal condition for growing CZTS, is necessary.[13] If Cu_{Zn} were responsible for the *p*-type self-doping, such a condition would be unfavorable because it suppresses the formation of Cu_{Zn} and therefore reduces the conductivity. Third, the origin of the native *p*-type conductivity is still under debate. For example, Cu vacancies (V_{Cu}) are still conjectured by some researchers to be the dominant acceptors in CZTS (Ref. 18) because of the Cu-poor growth condition.

In this paper, we study the intrinsic defects in CZTS based on hybrid functional calculations, which improve the description on thermodynamic and electronic properties of semiconductors. First, we show that CZTS is a thermodynamic stable material and no defects in our calculation have negative formation energy. Furthermore, we identify the Sn_{Zn} antisite and the defect complex $(Cu_3)_{Sn}$ as the major deep traps of minority carriers in CZTS (i.e., electrons). With this result, the optimal growth condition found in experiment can be clearly understood; i.e., the Cu-poor and Zn-rich conditions are to suppress the $(Cu_3)_{Sn}$ and Sn_{Zn} defects, respectively, in the growth. Except these two defects, no other defects can play a significant role as recombination centers. In particular, sulfur vacancy V_S, a low-formation-energy defect, does not exhibit any transition levels inside the band gap and therefore is electrically benign. We found that this counterintuitive behavior of V_S is because of rehybridization of the Sn atom next to V_S. Last, we show that depending on the growth condition either Cu_{Zn} or V_{Cu} may contribute the majority of hole carriers. Particularly, under the growth condition that minimizes the deep electron traps, V_{Cu} dominates the hole carriers over Cu_{Zn}.

II. METHOD

Our hybrid functional calculations were carried out using the VASP package.[19] We employed the Heyd-Scuseria-Ernzerhof (HSE06) functional,[20,21] which mixes 25% of screened Hartree-Fock exchange to the Perdew-Burke-Ernzerhof (PBE) exchange functional.[22] The screening parameter was set to 0.2 $Å^{-1}$. Projector augmented-wave

 ©2013 American Physical Society

potentials[23,24] were used to describe the core electrons. The cutoff energy for the plane-wave basis was set to 272 eV. This setup yields a band gap of 1.49 eV for CZTS in good agreement with the experimental value, 1.49–1.51 eV.[1,4] The supercell approach was used to model the defects. The supercell size and the corresponding k-point sampling will be described later. The atomic structures were optimized until the Hellman-Feynman forces on all atoms were smaller than 0.05 eV/Å. For complex defects, such as Cu clusters, we used the simulated annealing method[25] with the PBE calculation to obtain an initial structure.

The formation energy of a defect α of charge q is defined as[26]

$$\Delta H_{\mathrm{f}}^{q}(\alpha) = E(\alpha,q) - E(\mathrm{host}) + \sum_i n_i(E_i + \mu_i) + q(\epsilon_{\mathrm{VBM}} + \epsilon_{\mathrm{F}}), \quad (1)$$

where $E(\alpha,q)$ is the total energy of the supercell containing a defect α carrying a charge q, $E(\mathrm{host})$ is the total energy of a defect-free supercell of the host, ϵ_{F} is the Fermi energy measured from the valence-band maximum (VBM) denoted by ϵ_{VBM}, μ_i is the chemical potential measured with respect to the total energy per atom in the stable phase of element i denoted by E_i, and n_i is the number of atom i being exchanged during defect formation between the host and the atomic reservoir of energy $E_i + \mu_i$. For example, $n_{\mathrm{S}} = 1$ for the creation of a sulfur vacancy. The key to using Eq. (1) is to determine the range of the variables ϵ_{F} and μ_i. The Fermi energy ϵ_{F} typically varies between the VBM and conduction-band minimum. However, the determination of the allowed region for μ_i can be complicated by the existence of a handful of secondary phases.

III. RESULTS AND DISCUSSION

We consider that the defects are in equilibrium with CZTS, which means

$$2\mu_{\mathrm{Cu}} + \mu_{\mathrm{Zn}} + \mu_{\mathrm{Sn}} + 4\mu_{\mathrm{S}} = E_{\mathrm{Cu_2ZnSnS_4}} - (2E_{\mathrm{Cu}} + E_{\mathrm{Zn}} + E_{\mathrm{Sn}} + 4E_{\mathrm{S}}), \quad (2)$$

where $E_{\mathrm{Cu_2ZnSnS_4}}$ is the total energy per formula of CZTS. This condition leaves us with three independent variables. Here, we use μ_{Cu}, μ_{Zn}, and μ_{Sn}, which span a three-dimensional chemical-potential space. In addition to Eq. (2), to avoid the formation of secondary phases, it also needs to be satisfied that the sum of the chemical potentials of the constituent elements of a secondary phase is smaller than the formation energy of that phase.[15,16] Figure 1(a) shows the polyhedron, within which CZTS is thermodynamically stable. To obtain Fig. 1(a), we used the formation energies of secondary phases calculated using the HSE06 functional, as shown in Table I. In general, the formation energy obtained from HSE06 is larger and in better agreement with experiment than that from PBE (see Table I). One exception is SnS, for which HSE06 gives a slightly smaller formation energy than PBE.

In Fig. 1(a), the stable region of CZTS is bounded by the respective stable regions of the elemental phases, as well as the secondary compound phases. The region is in a thin-blade shape with a thickness of 0.15 eV only. It shares most of its boundaries with the Cu_2SnS_3 phase on the left (Zn poor) and

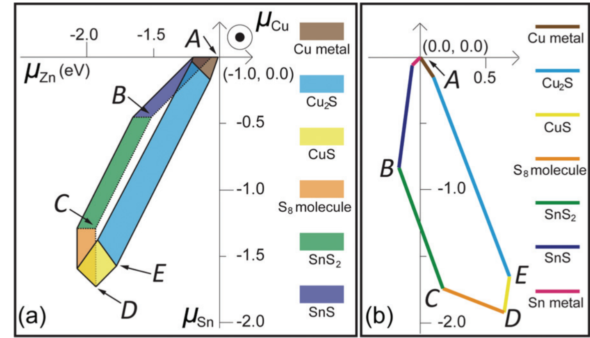

FIG. 1. (Color online) (a) Calculated stable region of CZTS in the chemical potential space spanned by μ_{Cu}, μ_{Zn}, and μ_{Sn}. Color-coded border planes indicate secondary phases that restrict the stable CZTS phase. For clarity, major secondary phases, Cu_2SnS_3 (to the left of the polyhedron) and ZnS (to the right of the polyhedron) are not colored. (b) A simplified view of the polyhedron in (a). Because the polyhedron has a thin-blade shape, one may approximate it by the interface with the ZnS phase, thereby reducing the three-dimensional polyhedron to a two-dimensional polygon.

the ZnS phase on the right (Zn rich). This result suggests that Cu_2SnS_3 and ZnS are easier to form than other secondary phases in the process of growing CZTS due to nonuniform control of chemical potentials. By viewing along the direction perpendicular to the blade, as shown in Fig. 1(b), the shape of the stable region of CZTS can be seen more clearly.

After establishing the stable region of CZTS in the chemical-potential space, we proceed to study the intrinsic defects in this material based on Eq. (1). To facilitate our discussion, we have labeled five points in Fig. 1, A–E, to represent the change in chemical potentials. Table II lists the chemical-potential values at these points. We first calculated the defect formation energies of neutral defects. In these calculations, we used a 64-atom supercell and two k points, Γ and $(\frac{1}{2}, \frac{1}{2}, \frac{1}{2})$, for the Brillouin-zone integration. For four defects, namely, $\mathrm{Cu_{Zn}}$, V_{Cu}, $\mathrm{Zn_{Cu}}$, and $\mathrm{Sn_{Zn}}$, we compared the results with those obtained using a larger 192-atom supercell. The comparison suggested that the results from the 64-atom supercell were converged to within 0.1 eV.

Figure 2 shows the formation energies calculated at points A–E. We studied in total 21 defects. For clarity, however,

TABLE I. Formation energy (in eV per formula) of secondary phases of CZTS calculated using PBE and HSE06 functionals: fcc Cu, hcp Zn, gray Sn, and S_8 molecules are used as the reference states. Available experimental results (Ref. 27) are listed for comparison.

	PBE	HSE06	Exp.
CuS	−0.41	−0.51	−0.55
Cu_2S	−0.41	−0.86	−0.82
ZnS	−1.63	−1.94	−2.14
SnS	−0.92	−0.87	−1.04
SnS_2	−1.16	−1.29	−1.45
Cu_2SnS_3	−2.04	−2.61	–
Cu_3SnS_4	−2.76	−3.05	–
Cu_4SnS_4	−2.28	−3.39	–
CZTS	−3.73	−4.69	–

TABLE II. Chemical-potential values at the representative points labeled in Fig. 1 in units of eV.

	μ_{Cu}	μ_{Zn}	μ_{Sn}
A	0	−1.02	0
B	−0.52	−1.52	−0.45
C	−0.73	−1.94	−1.29
D	−0.51	−1.94	−1.73
E	−0.35	−1.78	−1.57

only the defects that have formation energy lower than about 1.5 eV are shown. In Fig. 2, we see no negative formation energy, which is different from the results obtained using semilocal functionals in previous studies. Considering the fact that CZTS has been routinely synthesized at ambient condition, we believe that CZTS is a thermodynamically stable material, as also evidenced from our results. To understand why semilocal functionals might be inadequate for defect study, in Fig. 3 we compare the stable regions of CZTS as obtained from the HSE06 and PBE functionals. A different perspective from Fig. 1 has been used here. In both cases, the shaded area is where the Cu_3SnS_4 phase is more stable than CZTS. While this secondary phase has no effect on CZTS in the HSE06 result, it completely eliminates the stable region of CZTS in the PBE result. This explains why the Cu_{Zn} antisite always has negative formation energy in the PBE calculation.

In addition to the defects studied previously, we found that Cu atoms can form small clusters at a Zn or Sn vacancy site. The split interstitial, $(Cu_2)_{Zn}$, can have formation energy as low as 0.6 eV. In fact, the compound Cu_4SnS_4 by itself is a stable compound,[28] which is a semiconductor having a band gap of 0.82 eV at the Γ point according to our HSE06 calculation. Interestingly, we found that a Sn vacancy site can accommodate up to four Cu atoms, while the formation energy can be as low as 1.15 eV. Similar Cu clusters were proposed to exist in other semiconductor materials, such as silicon.[29,30] Because $(Cu_2)_{Zn}$ and $(Cu_4)_{Sn}$ are both fully compensated defects, they have no effect on the carrier concentration and recombination. Similarly, the low-formation-energy defect pairs, such as $Cu_{Zn} + Zn_{Cu}$, are also fully compensated. We will not discuss these defects further.

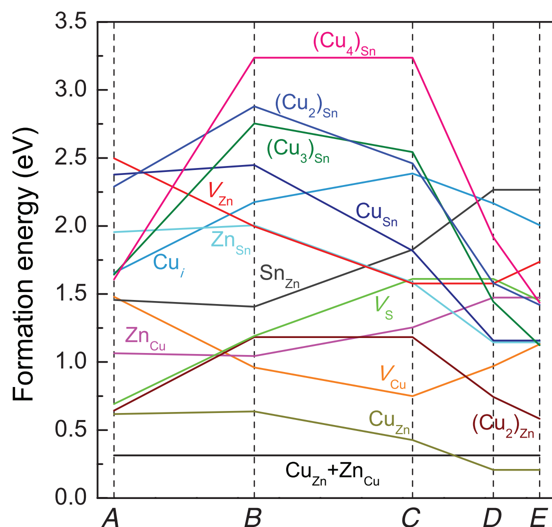

FIG. 2. (Color online) Calculated formation energy of intrinsic defects in CZTS as a function of chemical potentials at points A–E labeled in Fig. 1.

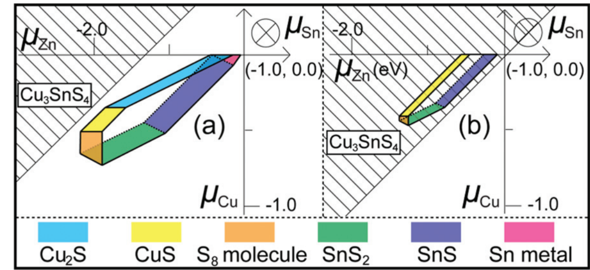

FIG. 3. (Color online) Comparison of the stable region of CZTS in the chemical potential space calculated from the hybrid HSE06 and semilocal PBE functionals. In the HSE06 result shown in (a), the stable Cu_3SnS_4 phase (shaded region) has no effect on the stable region of CZTS. In contrast, in the PBE result shown in (b), the stable Cu_3SnS_4 phase completely eliminates the CZTS region.

After a prescreening of the defects, we identify that the electrically active defects that have low formation energy in CZTS are Cu_{Zn}, Zn_{Cu}, Zn_{Sn}, Sn_{Zn}, $(Cu_m)_{Sn}$ with $m = 1$–3, V_{Cu}, V_S, and Cu_i. Here, we consider defects with ΔH_f lower than about 1.5 eV so that they can be incorporated in a significant amount during growth.[31] We calculated the transition levels for these low-formation-energy defects. The defect transition level, $\varepsilon(q/q')$, for a charge state transition from q to q', was defined as the Fermi energy ϵ_F in Eq. (1), at which $\Delta H_f^q = \Delta H_f^{q'}$. Note that $\varepsilon(q/q')$ does not depend on the chemical potentials. For the calculations where $q \neq 0$, one needs to correct the interaction of the charge q with its periodic images. The leading term of this interaction always lowers the total energy of the system. As a result, after correcting this error, the total energy of a charged state becomes higher, which means a deeper defect transition level because the neutral charge state is not affected by this problem. In our calculation, we first used the 64-atom supercell to calculate the defect transition levels. For three defects (Cu_{Zn}, V_{Cu}, and Zn_{Cu}), to further check the accuracy of our calculation, we used a 192-atom supercell and the Γ point representing the Brillouin zone. The above-mentioned error was corrected by an extrapolation from the results using 192-, 512-, and 1728-atom supercells and the PBE functional. The corrections were then applied to the HSE06 results obtained using the 192-atom supercell. It is worth noting that, compared with the results by extrapolation to an infinitely large supercell, the error in calculated transition levels even using a 64-atom supercell is smaller than 70 meV.

The calculated defect transition levels are shown in Fig. 4. Based on these results, we conclude that only $(Cu_3)_{Sn}$ and Sn_{Zn} can be effective electron traps in CZTS. Other defects have either only shallow levels, so that the captured electrons can be easily thermoexcited back to the conduction band, or only negatively charged deep levels, which repel electrons. According to previous semilocal functional calculations, V_S has a $(0/2+)$ transition level in the middle of the band gap and therefore could be a major electron trap in CZTS. However, our result shows that V_S does not have any defect transition levels inside the band gap, indicating that it is an electrically

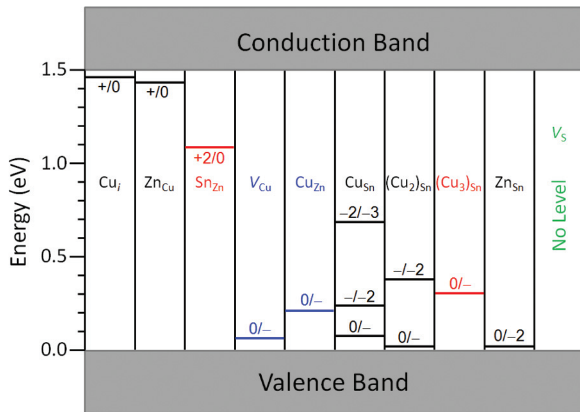

FIG. 4. (Color online) Calculated defect transition levels in CZTS using the HSE06 functional. The deep electron traps are marked in red, while the important acceptors are marked in blue. Note that V_S does not introduce any transition levels in the band gap.

benign defect. Our analysis shows that the Sn atom next to the vacancy site undergoes a transition of valence state from 4+ to 2+, which is accompanied by a significant displacement of the Sn atom towards the vacancy site. This valence state change of the Sn atom is equivalent to a double acceptor, which fully compensates the V_S double donor. We note that this rehybridization process can also be described by the semilocal functionals. But the uncertainty introduced by correcting the band-gap error in such calculations could give rise to the defect transition level in the band gap.

Our identification of deep traps in CZTS is consistent with the optimal growth conditions of CZTS for high-PCE solar cells,[13] which are the following: (1) the chemical composition ratio of Cu and Sn, [Cu]/[Sn], in the precursor is about 1.7–1.8, i.e., a Cu-poor condition compared with the stoichiometric ratio of 2; (2) the Zn to Sn ratio [Zn]/[Sn] is about 1.2–1.3, i.e., a Zn-rich condition compared with the stoichiometric ratio of 1. According to our results, such conditions can be clearly understood, where condition 1 corresponds to the suppression of the $(Cu_3)_{Sn}$ defects and condition 2 corresponds to the suppression of the Sn_{Zn} defects. We note that the nonstoichiometric precursor used in the experiments inevitably leads to the formation of secondary phases. As a result, the CZTS domains in actual samples are not significantly off-stoichiometric as in the precursor. It has been reported that a significant amount of the ZnS phase in CZTS could degrade the solar-cell performance.[32] Another major secondary phase Cu_2SnS_3 in the orthorhombic $Imm2$ structure[33] has a band gap of 0.66 eV from our HSE06 calculation, which may limit the open-circuit voltage in a CZTS-based solar cell. Therefore, fine tuning of the growth condition to reach a best compromise between the minimization of deep traps and secondary phases is necessary for further improving the PCE.

Finally, we estimate the hole concentration in CZTS based on our calculated formation energies and transition levels. As can be seen from Fig. 2, $(Cu_3)_{Sn}$ and Sn_{Zn} have the lowest formation energy in the regions from point D to E and A to B, respectively. To avoid these deep traps, the preferred growth condition would be at point C, where both defects have relatively high formation energy. The calculated formation energies for Cu_{Zn} and V_{Cu} at point C are 0.43 and 0.75 eV, respectively. We consider that the defects are incorporated at the growth temperature (540 °C) and then frozen in the material. Using the calculated transition level $\varepsilon(0/-)$, which is 217 meV for Cu_{Zn} and 66 meV for V_{Cu}, we obtained the hole concentration of 4×10^{15} cm^{-3} due to Cu_{Zn} and 3×10^{16} cm^{-3} due to V_{Cu}. So, even though the concentration of Cu_{Zn} (2×10^{19} cm^{-3}) in CZTS is much higher than that of V_{Cu} (4×10^{17} cm^{-3}), the majority of the hole carriers could still be contributed by V_{Cu} because of the much shallower transition level of V_{Cu}. On the other hand, if the growth condition favors the formation of Cu_{Zn}, the roles of these two acceptors will switch. For example, at point D, Cu_{Zn} contributes 8×10^{16} cm^{-3}, while V_{Cu} contributes only 2×10^{15} cm^{-3} hole carriers. Even though the estimated concentrations could vary by up to one order of magnitude due to the uncertainties in our calculation, we found that our estimated hole concentrations at both points C and D are consistent with reported experimental values, which usually fall in the range from 10^{16} to 10^{17} cm^{-3}.[4,13,18]

IV. CONCLUSIONS

In summary, our hybrid functional calculations reveal the key intrinsic defects in CZTS. The Sn_{Zn} antisite and the defect complex $(Cu_3)_{Sn}$ are found to be the main deep electron traps. Our results provide a microscopic understanding on the optimal growth condition of CZTS. Under the optimal growth condition, V_{Cu} could contribute the majority of the hole carriers, even though its concentration is much lower than another acceptor Cu_{Zn}. In addition, no defects in our calculations show negative formation energy, indicating that CZTS is a thermodynamically stable material.

ACKNOWLEDGMENTS

The authors would like to thank S.-H. Wei, B. Shin, D. Mitzi, S. Guha, L. Deligianni, X.-G. Gong, and S. Chen for helpful discussions. This work was supported by National Science Foundation (NSF) under Grant No. DMR-1104994 and the Department of Energy (DOE) under Grant No. DE-SC0002623. The work at Jilin University (JLU) was supported by National Natural Science Foundation of China (NSFC) (Grant No. 11104109). The supercomputer time was provided by National Energy Research Scientific Computing Center (NERSC) under the DOE Contract No. DE-AC02-05CH11231, the Computational Center for Nanotechnology Innovations (CCNI) at Rensselaer Polytechnic Institute (RPI), and the High Performance Computing Center (HPCC) at JLU.

*Email:suny4@rpi.edu
†Email:zhangs9@rpi.edu
[1] J.-S. Seol, S.-Y. Lee, J.-C. Lee, H.-D. Nam, and K.-H. Kim, Sol. Energ. Mat. Sol. Cells **75**, 155 (2003).
[2] K. Jimbo, R. Kimura, T. Kamimura, S. Yamada, W. S. Maw, H. Araki, K. Oishi, and H. Katagiri, Thin Solid Films **515**, 5997 (2007).
[3] H. Katagiri, K. Jimbo, S. Yamada, T. Kamimura, W. S. Maw, T. Fukano, T. Ito, and T. Motohiro, Appl. Phys. Express **1**, 041201 (2008).

[4]J. J. Scragg, P. J. Dale, and L. M. Peter, Electrochem. Comm. **10**, 639 (2008).
[5]H. Katagiri, K. Jimbo, W. S. Maw, K. Oishi, M. Yamazaki, H. Araki, and A. Takeuchi, Thin Solid Films **517**, 2455 (2009).
[6]S. Chen, X. G. Gong, A. Walsh, and S.-H. Wei, Appl. Phys. Lett. **94**, 041903 (2009).
[7]J. Paier, R. Asahi, A. Nagoya, and G. Kresse, Phys. Rev. B **79**, 115126 (2009).
[8]T. K. Todorov, K. B. Reuter, and D. B. Mitzi, Adv. Mater. **22**, E156 (2010).
[9]K. Wang, B. Shin, K. B. Reuter, T. Todorov, D. B. Mitzi, and S. Guha, Appl. Phys. Lett. **98**, 051912 (2011).
[10]D. A. R. Barkhouse, O. Gunawan, T. Gokmen, T. K. Todorov, and D. B. Mitzi, Prog. Photovolt. Res. Appl. **20**, 6 (2012).
[11]A. Walsh, S. Chen, S.-H. Wei, and X.-G. Gong, Adv. Energy Mater. **2**, 400 (2012).
[12]K. Wang, O. Gunawan, T. Todorov, B. Shin, S. J. Chey, N. A. Bojarczuk, D. Mitzi, and S. Guha, Appl. Phys. Lett. **97**, 143508 (2010).
[13]B. Shin, O. Gunawan, Y. Zhu, N. A. Bojarczuk, S. J. Chey, and S. Guha, Prog. Photovolt. Res. Appl. **21**, 72 (2013).
[14]T. K. Todorov, J. Tang, S. Bag, O. Gunawan, T. Gokmen, Y. Zhu, and D. B. Mitzi, Adv. Energy Mater. **3**, 34 (2013).
[15]S. B. Zhang, S.-H. Wei, A. Zunger, and H. Katayama-Yoshida, Phys. Rev. B **57**, 9642 (1998).
[16]S. Chen, J.-H. Yang, X. G. Gong, A. Walsh, and S.-H. Wei, Phys. Rev. B **81**, 245204 (2010).
[17]A. Nagoya, R. Asahi, R. Wahl, and G. Kresse, Phys. Rev. B **81**, 113202 (2010).
[18]A. Nagaoka, K. Yoshino, H. Taniguchi, T. Taniyama, and H. Miyake, J. Crys. Growth **341**, 38 (2012).
[19]G. Kresse and J. Furthmüller, Comput. Mater. Sci. **6**, 15 (1996).
[20]J. Heyd, G. E. Scuseria, and M. Ernzerhof, J. Chem. Phys. **118**, 8207 (2003).
[21]J. Heyd, G. E. Scuseria, and M. Ernzerhof, J. Chem. Phys. **124**, 219906 (2006).
[22]J. P. Perdew, K. Burke, and M. Ernzerhof, Phys. Rev. Lett. **77**, 3865 (1996).
[23]P. E. Blöchl, Phys. Rev. B **50**, 17953 (1994).
[24]G. Kresse and D. Joubert, Phys. Rev. B **59**, 1758 (1999).
[25]S. Kirkpatrick, C. D. Gelatt, Jr., and M. P. Vecchi, Science **220**, 671 (1983).
[26]S. B. Zhang and J. E. Northrup, Phys. Rev. Lett. **67**, 2339 (1991).
[27]D. R. Lide, *CRC Handbook of Chemistry and Physics*, 84th ed. (CRC, Boca Raton, 2003).
[28]S. Jaulmes, J. Rivet, and P. Laruelle, Acta Cryst. B **33**, 540 (1977).
[29]M. Steger, A. Yang, N. Stavrias, M. L. W. Thewalt, H. Riemann, N. V. Abrosimov, M. F. Churbanov, A. V. Gusev, A. D. Bulanov, I. D. Kovalev, A. K. Kaliteevskii, O. N. Godisov, P. Becker, and H. J. Pohl, Phys. Rev. Lett. **100**, 177402 (2008).
[30]A. Carvalho, D. J. Backlund, and S. K. Estreicher, Phys. Rev. B **84**, 155322 (2011).
[31]Using the experimental annealing temperature of 540 °C, for example, we estimate that the formation energy of 1.5 eV corresponds to 3.5×10^{12}-cm^{-3} Zn- or Sn-site defects.
[32]J. Just, D. Lützenkirchen-Hecht, R. Frahm, S. Schorr, and T. Unold, Appl. Phys. Lett. **99**, 262105 (2011).
[33]Y.-T. Zhai, S. Chen, J.-H. Yang, H.-J. Xiang, X.-G. Gong, A. Walsh, J. Kang, and S.-H. Wei, Phys. Rev. B **84**, 075213 (2011).